Histol Histopathol (2002) 17: 789-798

http://www.hh.um.es

Histology and Histopathology

Cellular and Molecular Biology

Expression of ribosomal protein L4 (rpL4) during neurogenesis and 5-azacytidine (5AzC)-induced apoptotic process in the rat

M. Ueno[1], H. Nakayama[1], S. Kajikawa[2], K. Katayama[1], K. Suzuki[1] and K. Doi[1]

[1]Department of Veterinary Pathology, Graduate School of Agricultural and Life Sciences, The University of Tokyo, Bunkyo-ku, Tokyo, Japan and [2]Safety Research Laboratories, Yamanouchi Pharmaceutical Co., Ltd., Itabashi-ku, Tokyo, Japan

Summary. 5-Azacytidine (5AzC) induces neuronal apoptosis in rat and mouse fetuses. 5AzC also induces apoptosis in undifferentiated PC12 cells, and ribosomal protein L4 (rpL4) mRNA expression increases prior to apoptosis. To clarify the roles of rpL4 during neurogenesis, we first examined the distribution of rpL4 mRNA in the developing rat brain by *in situ* hybridization and RT-PCR, and compared the results to the distribution of TUNEL- or PCNA-positive cells. rpL4 mRNA expression was strong in the ventricular zone (VZ), subventricular zone (SVZ), cortical plate (CP), cerebral cortex, granule cell layer (GCL), pyramidal cell layer (Py) and external granular layer (EGL) during embryonic and early postnatal days, and it was remarkably weakened thereafter. A lot of PCNA-positive cells were observed in VZ, SVZ, and EGL during embryonic and early postnatal days, and such distribution of PCNA-positive cells was almost identical to rpL4 mRNA distribution. Only few TUNEL-positive cells were observed in VZ, SVZ, cerebral cortex, EGL, and hippocampus during embryonic and early postnatal days, and the regions with TUNEL-positive cells were not identical to rpL4 mRNA distribution. Next, the changes of rpL4 mRNA expression in the brain of 5AzC-treated rat fetuses were examined by *in situ* hybridization and RT-PCR. Apoptotic cells appeared at 9 to 24 hours after treatment (HAT). However, the rpL4 mRNA expression was unchanged during the apoptotic process. From the results, it is suggested that rpL4 would have certain roles in cell proliferation and differentiation during neurogenesis, but have no roles in 5AzC-induced apoptosis in the fetal brain.

Key words: Rat, Ribosomal protein L4 (rpL4), 5-Azacytidine, Brain development, Apoptosis

Offprint requests to: Masaki Ueno, Department of Veterinary Pathology, Graduate School of Agricultural and Life Sciences, The University of Tokyo, 1-1-1 Yayoi, Bunkyo-ku, Tokyo 113-8657, Japan. Fax: +81-3-5841-8185. e-mail: a80502@mail.ecc.u-tokyo.ac.jp

Introduction

Ribosome is known as an intracytoplasmic organella involved in protein synthesis, consisting of rRNA and approximately 80 kinds of ribosomal proteins (rp) (Wool et al., 1995). Ribosomal protein L4 (rpL4) is a protein of 47,280 molecular weight, composing the large unit of rp (Chan et al., 1995), but its function remains unknown except for a ribosomal component. Protein synthesis is active in the proliferation phase of cells, and rp synthesis is assumed to be active at the phase. Actually, the expression of several rps (L5, L7, L32, and S16) at both transcription and translation levels was high in the liver of rat fetuses, and the levels were lower in adult liver. The expression was increased again in the regenerative liver following partial hepatectomy (Aloni et al., 1992). In addition, the increased rp expression was also observed during cell differentiation. For example, translation of rpL4 in PC12 cells, a cell line derived from rat pheochromocytoma, was repressed after they completely finished the differentiation toward neurons by NGF treatment, but promoted again during neurite regeneration by shearing neurites (Twiss et al., 2000). Therefore, rp expressions are presumed to be elevated during either cell proliferation or differentiation. In addition, Kajikawa et al. (1998) reported that increased expression of rpL4 mRNA was detected prior to apoptosis of 5-azacytidine (5AzC)-treated PC12 cells. Therefore, the protein may also be involved in the mechanism of neuronal apoptosis.

5AzC is a cytidine analogue which possesses a nitrogen atom instead of a carbon atom at the 5 position of the pyrimidine ring. It was synthesized in 1964 (Sorm et al., 1964) as a cancer therapeutic agent. At present, however, it is only used for chemotherapy of acute myeloid leukemia and myelodysplastic syndrome (Pinto and Zagonel, 1993; Cheson et al., 2000), because of the unstable effects among patients and major side effects. It is said that 5AzC promotes differentiation of the mouse embryo C3H 10T1/2 C18 cells to striated muscles (Constantinidis et al., 1977), and that it promotes the

fetal hemoglobin synthesis in the erythrocytes (Charache et al., 1983). 5AzC may also activate apoptotic processes and induce cell toxicity in tumor cells (Murakami et al., 1995; Bender et al., 1998; Hara et al., 1998; Wang et al., 1998), mouse fetal brain cell culture and PC12 cells (Hossain et al., 1996, 1997a,b), and in rat and mouse fetal brain (Hossain et al., 1995; Lu et al., 1998), probably due to its DNA hypomethylating effect (Bender et al., 1998) or to covalent binding of DNA-cytosine methyltransferase with 5AzC containing DNA (Santi et al., 1984; Michalowsky and Jones, 1987).

Cell proliferation, differentiation, and following exclusion of excess cells by apoptosis in the developing central nervous system are well known evidences. We, therefore, supposed that rpL4 might play some crucial roles in the development of the central nervous system, such as exclusion of excess neuronal cells by apoptosis or switching the cells from proliferation to differentiation.

In the present study, the expression of rpL4 mRNA in the developing rat brain was first examined by *in situ* hybridization and reverse transcription–polymerase chain reaction (RT-PCR) methods, and proliferative activities and physiological apoptosis of developing brain cells were further investigated. Next, 5AzC was injected into pregnant rats to induce apoptosis in the fetal brain, and the relationship between the expression of rpL4 mRNA and the development of 5AzC-induced neuronal apoptosis was sequentially examined.

The Laboratory Animal Use and Care Committee of the Graduate School of Agricultural and Life Sciences, the University of Tokyo, approved the present study.

Materials and methods

Animals and chemicals

Jcl:Wistar rats were obtained from Japan CLEA, Tokyo, Japan. Animals were kept in isolated cages under a semi-controlled condition (23±2 °C with 55±5% humidity and a 14-hr light/10-hr dark cycle) and fed commercial pellets (MF; Oriental Yeast, Tokyo, Japan) and water *ad libitum*. 5AzC (Sigma, St. Louis, MO) was dissolved in physiological saline (5 mg/ml) immediately before administration.

Experimental designs

Three pregnant rats were sacrificed by heart puncture under diethyl ether anesthesia at 13, 15, 18, and 21 day of gestation (E13, 15, 18, and 21), respectively, and fetuses were collected. Six rats were sacrificed in the same way at postnatal days 1, 4, 7, 14, 21, 28, 56, 84, and 252 (P1, 4, 7, 14, 21, 28, 56, 84, and 252), respectively, and brains were collected. The fetal heads were cut at the sagittal line, and postnatal brains at the sagittal or the transverse line including lateral ventricle, hippocampus, and cerebellum, respectively. They were embedded in O.C.T. compound (Sakura, Tokyo, Japan) and kept at -80 °C until use. Frozen sections (6 μm thick) were subjected to *in situ* hybridization, TdT mediated dUTP nick end labeling (TUNEL) method, and proliferating cell nuclear antigen (PCNA) immunohistochemistry. Additional head and brain tissues were directly frozen at -80 °C for extraction of total RNA and further RT-PCR method.

Eighteen pregnant rats at gestation day 13 were injected with 10 mg/kg of 5AzC intraperitoneally (i.p.), and 3 rats were sacrificed at 1, 3, 6, 9, 12, and 24 hours after treatment (HAT), respectively. The dose of 5AzC was selected according to the previous experiments in which the dose caused a high induction of neuronal apoptosis and a low fetal mortality (Lu et al., 1998). As controls, three pregnant rats were injected with 2 ml/kg of physiological saline and sacrificed at 1HAT. The fetuses were subjected to *in situ* hybridization and RT-PCR to detect rpL4 mRNA expression as described below. Some fetuses were fixed in 10% neutral-buffured formaline, and paraffin sections (4 μm thick) were stained with hematoxylin and eosin (HE) or by the TUNEL method.

rpL4 probe

rpL4 cDNA cloned from cDNA library of 5AzC-treated PC12cells (Kajikawa et al., 1998) was inserted into pBluescript SK- plasmid (STRATAGENE, Austin, TX). The 375 bp sequence from nt 848 to nt 1222 of rat rpL4 cDNA (Fig. 1) was amplified from the plasmid by PCR (denaturation at 95 °C for 1 min, annealing at

848-cacaagatgatgaacacagaccttagcagaatcttgaaaagcccagagatccaaagagcccttcgagca
ccacgcaagaagattcatcgcagagtcttgaagaagaatccactgaagaatctgaggatcatgttgaagctgaac
ccttacgcaaagactatgcgtaggaacaccattctccgccaggctaggaatcacaaacttcgagtgaaaaagctg
gaagccgcagctgctgcactggcagccaaatcggagaagattgttccagagaaggggctggagacaaaaaacc
tgcagtaggcaaaaaaggaaagaagcctgtggatgccaagaagctgaagaagcctgcagggaaaaaggtggtta
ccaagaaac-1222

Fig. 1. Rat rpL4 cDNA sequence used as a probe.

Table 1. Primer sequences used in PCR.

PRODUCT	UPPER PRIMER	LOWER PRIMER
rpL4	CACAAGATGATGAACACAGA	GTTTCTTGGTAACCACCTTTTTCC
rpL4 including T7 promotor	GATCCTAATACGACTCACTATAGGGAGG CACAAGATGATGAACACAGA	GGATCCTAATACGACTCACTATAGGGAGG GTTCTTGGTAACCACCTTTTTCC
GADPH	GAGTATGTCGTGGAGTCTACTG	GCTTCACCACCTTCTTGATGTC

50 °C for 1 min, and extension at 72 °C for 1 min: 30 cycles) using the oligonucleotide primers set shown in Table 1. The obtained PCR products were electrophoresed in 2 % agarose S (Nippon Gene, Toyama, Japan) / 1xTAE buffer (40 mM Tris-aminomethane, 40 mM glacial acetic acid, 1 mM EDTA) and rpL4 cDNA at the 375 bp band was purified using GENECLEAN Kit (Qbiogene, Carlsbad, CA). To make cRNA probes, the extracted rpL4 cDNA was then amplified by PCR using the oligonucleotide primers set including T7 promoter sequence (Table 1; GGATCCTAATACGACTCACTATAGGGAGG). T7 transcription was performed using T7 RNA polymerase (STRATAGENE, Austin, TX) and DIG RNA labeling mix, x10 conc. (Roche, indianapolis, IN), and finally digoxigenin (Dig)-labeled cRNA probes were obtained.

In situ hybridization

Frozen brain sections (6 μm) were sequentially treated with 4% paraformaldehyde/PBS at 4 °C for 30 min, PBS at room temperature (RT) for 10 min, DEPC-DW for 5 min, 0.2 M HCl/DEPC-DW for 8 min, 0.1 M triethanolamine-HCl (pH 8.0) (TEA) for 1 min, 0.25 % acetic anhydride / TEA for 15 min, and 2xSSC (saline-sodium citrate buffer, 1xSSC: 150 mM NaCl, 15 mM sodium citrate, pH 7.2) at 50 °C for 10 min. After pretreatment with 50 % formamide/2xSSC at 50 °C for 1 hr, the sections were then hybridized at 50 °C for 18 hr in the probe solution (probe concentration: 2 μg/ml, including 40% deionized formamide, 10% dextran sulfate, 1xDenhardt's solution, 4xSSC, 10 mM DTT, 1 mg/ml yeast t-RNA, 0.1 mg/ml denatured and sheared salmon sperm DNA). The sections were then rinsed with 2xSSC at 50 °C for 10 min, washed with 50% formamide/2xSSC at 50 °C for 30 min and further incubated with TNE buffer (10 mM Tris-HCl (pH 7.6), 0.5 M NaCl, 1 mM EDTA) for 10 min , 10 μg/ml RNase A/TNE buffer, for 30 min and TNE buffer for 10 min, at 37 °C, respectively. The sections were then washed with 2xSSC for 30 min twice and 0.2xSSC for 30 min twice at 48 °C.

For signal detection, the sections were pretreated twice with buffer 1 (100 mM Tris-HCl (pH 7.5), 150 mM NaCl) for 10 min and blocking solution (1% blocking reagent/buffer 1) for 30 min, and then incubated with alkaline phosphatase-conjugated anti-Dig antibody (1:500, Roche, Mannheim, Germany)/blocking solution at 4 °C overnight. After washing twice with buffer 1 for 10 min and buffer 2 (100 mM Tris-HCl (pH 9.5), 100 mM NaCl, 50 mM $MgCl_2$) for 10 min, the signals were visualized with color solution (0.6 mM 4-nitro blue tetrazolium chloride (NBT), 0.4 mM 5-bromo-4-chloro-3-indolil-phosphate (BCIP)/buffer2).

RT-PCR

Total RNA was extracted from each homogenized brain sample using the Isogen kit (Nippon Gene). Reverse transcriptase (RT) reaction for the first strand cDNA synthesis was carried out using oligo (dT)12-18 primer and SUPERSCRIPT™ II RNase H- Reverse Transcriptase (Gibco, Gaithersburg, MD). PCR was performed using the oligonucleotide primer sets corresponding to the cDNA sequences of rpL4 or glyceraldehyde-3-phosphate dehydrogenase (GAPDH) (Table 1). In brief, 100 μl of reaction mixture containing 10 μl 10xPCR buffer (100 mM Tris-HCl buffer, 500 mM KCl, and 15 mM $MgCl_2$; Takara, Shiga, Japan), 10 μl dNTP (Takara), 50 pmol of both upper and lower primer, and 1 μg of the cDNA sample, was pre-heated at 95 °C for 5 min, and 21 cycles of PCR reaction (denaturation at 95 °C for 1 min, annealing at 50 °C (rpL4)/58 °C (GAPDH) for 1 min, and extension at 72 °C for 1 min) were performed using Takara PCR Thermal cycler SP (Takara). The PCR products were electrophoresed in 2 % agarose S (Nippon Gene)/1xTBE buffer (89 mM Tris-aminomethane, 89 mM Boric acid, 2 mM EDTA). The gels were stained with ethidium bromide (Gibco). Fluorescent bands were visualized using a UV-CCD video system (EpiLight UVFA1100; AISIN COSMOS, Tokyo, Japan) and were analyzed using an image-analysis software, Quantity One (pdi, NY) on a computer (Power Macintosh $8100/100_{AV}$). Relative intensity of rpL4 band against GAPDH band was calculated.

TUNEL method

Cells with DNA fragmentation (apoptotic cells) were detected by the TUNEL method first proposed by Gavrieli et al. (1992), using an apoptosis detection kit (Apop Tag; Intergen, Purchase, NY). In brief, multiple fragmented DNA 3'-OH ends on the section were labeled with digoxigenin-dUTP in the presence of terminal deoxynucleotidyl transferase (TdT). Peroxidase-conjugated anti-digoxigenin antibody was then reacted with the sections. Apoptotic nuclei were visualized by peroxidase-diaminobenzidine (DAB) reaction. The sections were then counterstained with methyl green.

Immunohistochemistry for PCNA

Immunohistochemical staining for PCNA was carried out by the avidine-biotin-peroxidase complex (ABC) method using the Vectastain Elite ABC Kit (Vector, Burlingame, CA). Mouse anti-PCNA monoclonal antibody (PC10; Novocastra, Newcastle upon Tyne, UK) and biotinylated goat anti-mouse IgG antibody (Kirkegaard & Perry, Gaitherburg, MD) were used as first and second antibodies, respectively. After ABC reaction, sections were colorized by peroxidase-DAB reaction. The sections were then counterstained with methyl green or hematoxylin.

Morphometry

The percentage of PCNA-positive cells and the thickness in the PCNA-positive regions, i.e. the

ventricular zone (VZ), subventricular zone (SVZ), external granular layer (EGL), and subgranular zone (SgZ) were used to evaluate the proliferative activities. The thickness of PCNA-positive region was represented by cell number. For counting PCNA-positive cells, two brains were randomly chosen at each day, respectively. PCNA-positive cells were counted in a randomly chosen field (x400) under a light microscope. The percentage and the thickness of PCNA-positive cells in each region were represented as the mean. For counting TUNEL-positive cells in the developing brains and 5AzC-treated fetuses, two brains were randomly chosen at each day, respectively. TUNEL-positive cells were counted in a randomly chosen field of each brain region (x400) under a light microscope. The percentage of TUNEL-positive cells was represented as the mean. The chosen brains or fetuses at each time were obtained from different dams.

Results

The expression of rpL4 mRNA in the rat brain

The results of RT-PCR are shown in Fig. 2. Strong expression of rpL4 mRNA was observed in embryo brains at E13 and 18. The expression in the cerebral cortex was continuously seen at the same level as that in embryos at P4, and decreased after P21 (Fig. 2a). The expression in the hippocampus was high at P7, and became significantly lower at P84 (Fig. 2b). In the cerebellum, high expression of rpL4 was observed at P4 and gradually decreased thereafter (Fig. 2c). In the brain stem, rpL4 was highly expressed at P4 and remarkably decreased after P21 (Fig. 2d). It was therefore concluded that the expression of rpL4 mRNA was high in the embryonic and neonatal days, and it remarkably decreased thereafter at any regions.

We then performed *in situ* hybridization to examine the distribution of rpL4 mRNA expression. The results are summarized in Table 2. In embryonic days, the rpL4 signals were continuously detected at high levels in VZ, SVZ, and cortical plate (CP) of telencephalon (Fig. 3a, c). During the several neonatal days, the expression was still observed at a high level in VZ, SVZ, and cerebral cortex (Fig. 4a,c), while it remarkably decreased after P21 (Fig. 4b). In the hippocampus, rpL4 mRNA was highly expressed in the granule cell layer of dentate gyrus (GCL) and pyramidal cell layer (Py) from P1 to P4, and it decreased thereafter (Fig. 5a,b). In the cerebellum, EGL was positive for rpL4 expression from E21 to P14, but the signals were not detected after P21 due to the disappearance of the layer (Fig. 6a,d). The internal granular layer (IGL) began to be formed at around P7, and weak signals were detected in the layer from P7 to P21. After that, the signals became weaker. Spatiotemporal distribution of rpL4 mRNA signals corresponded to the results of RT-PCR mentioned above.

Distribution of PCNA-positive cells in the rat brain

The distribution of PCNA-positive cells is

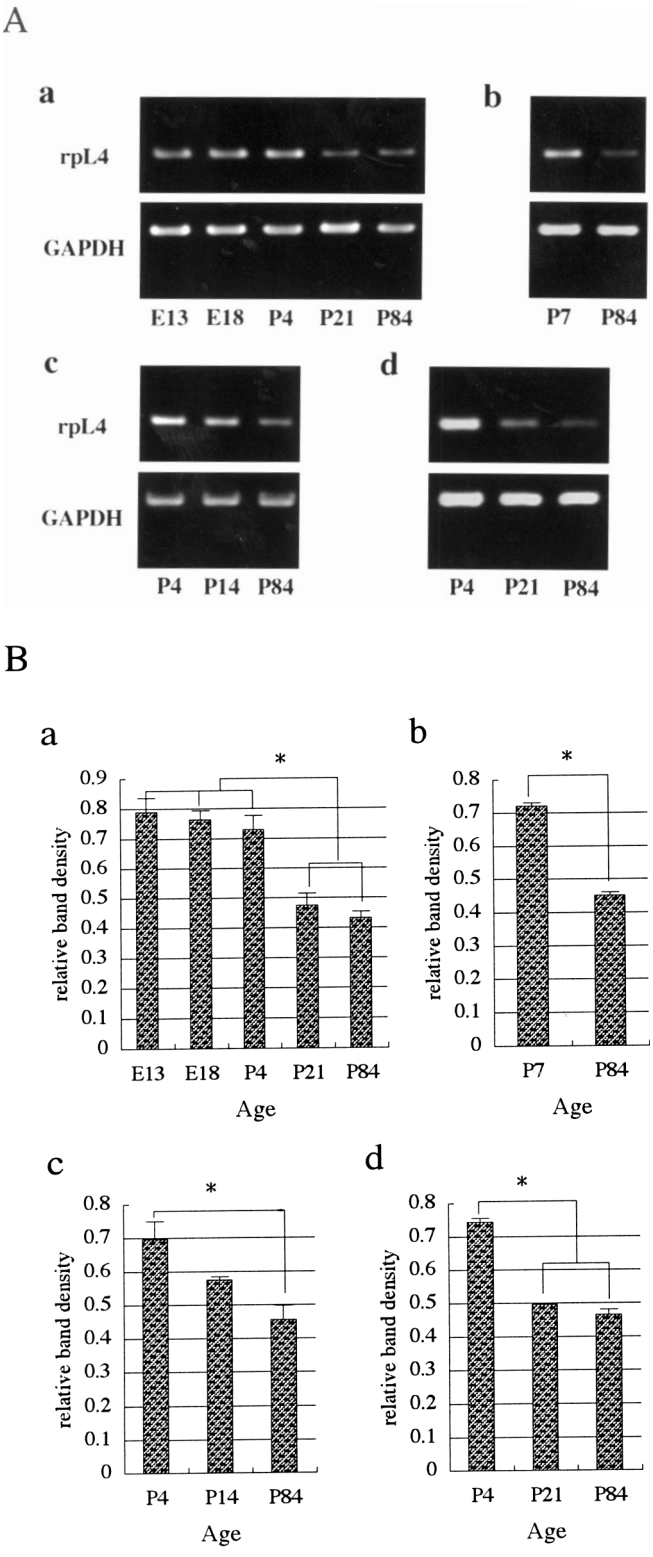

Fig. 2. The expression of rpL4 mRNA by RT-PCR. **A.** Agarose gel electrophoresis. **B.** The relative rpL4 band density to GAPDH. Each value represents mean±SD of 3 samples. a: Cerebral cortex (E13 and E18: the whole brain). b: Hippocampus. c: Cerebellum. d: Brain stem. *: Significant ($p<0.05$) by Fisher's PLSD test.

summarized in Table 3. A number of PCNA-positive cells were seen in VZ and SVZ from E13 to P14 (mainly VZ in embryonic days, and SVZ in postnatal days; Figs. 3d and 4d). The positive cells were also detected in cerebellar EGL from E21 to P14 (Fig. 6b). The PCNA-positive regions were identical to the areas of rpL4

Table 2. The expression of rpL4 mRNA in the rat brain by in situ hybridization.

AGE	CEREBRUM				HIPPOCAMPUS	CEREBELLUM	
E13	VZ (+)						
E15	VZ (++)						
E18	VZ (++)	SVZ (++)	CP (++)	IZ (±)			
E21	VZ (+)	SVZ (+)	CP (+)			EGL (+)	
P1	VZ (+)	SVZ (+)	cortex (+)		GCL, Py (+)	EGL (+)	
P4	VZ (+)	SVZ (+)	cortex (+)		GCL, Py (+)	EGL (+)	
P7	VZ (+~±)	SVZ (+~±)	cortex (+~±)		GCL, Py (±)	EGL (+~±)	IGL (+~±)
P14	VZ (±)	SVZ (±)	cortex (±)		GCL, Py (+~±)	EGL (+~±)	IGL (±)
P21			cortex (±)		GCL, Py (±)		IGL (±)
P28			cortex (±~-)		GCL, Py (±~-)		IGL, y (±~-)
P56			cortex (±~-)		GCL, Py (±~-)		IGL, y (±~-)
P84			cortex (±~-)		GCL, Py (±~-)		IGL, y (±~-)
P252			cortex (±~-)		GCL, Py (±~-)		IGL, y (±~-)

++: Strong signals; +: moderate signals; ±: weak signals; -: no signals.

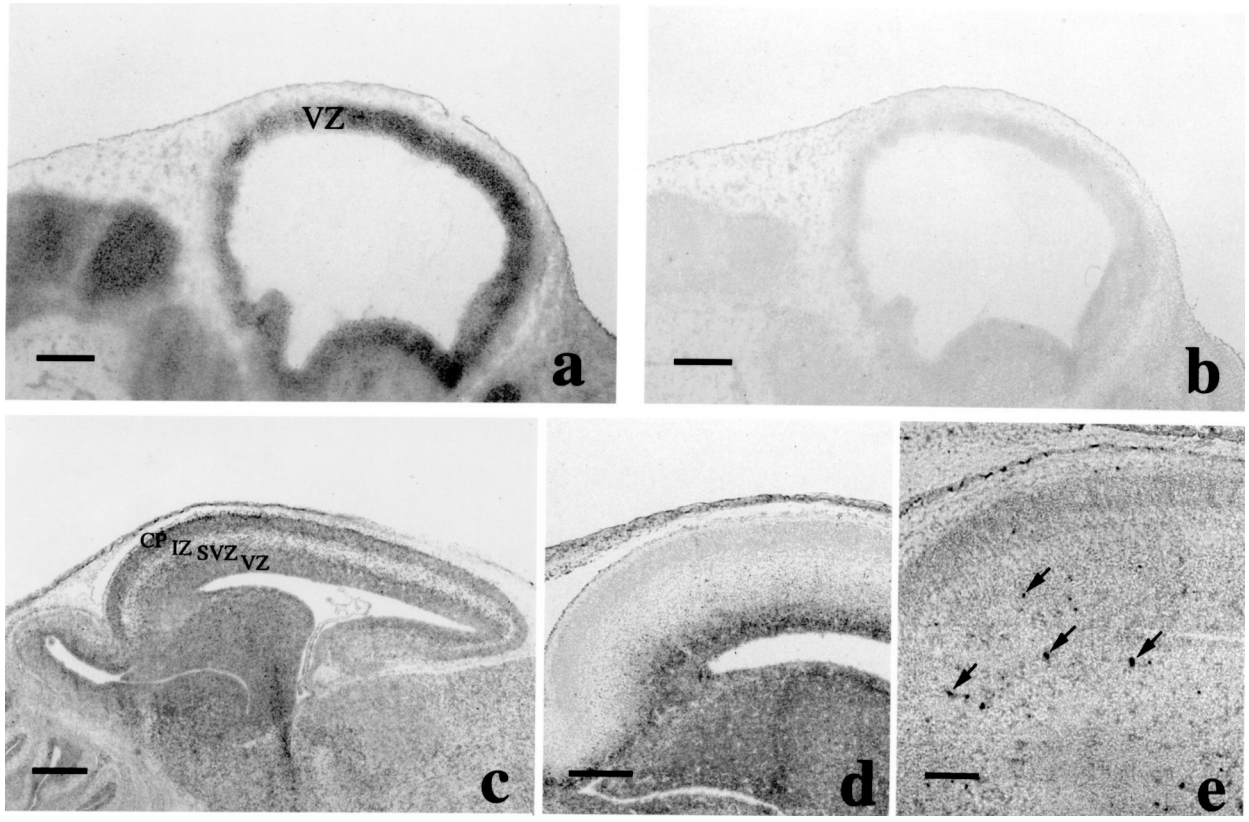

Fig. 3 . Distribution of rpL4 mRNA and PCNA- or TUNEL-positive cells in the telencephalon of rat fetuses. Telencephalons at E13 **(a and b)** and E18 **(c, d, and e)** are subjected to in situ hybridization with antisense probe **(a and c)** or sense probe **(b),** immunohistochemistry for PCNA **(d)** and TUNEL method **(e).** Bar: a,b; 300 μm, c,d; 600 μm, e; 200 μm.

Table 3. Distribution of PCNA-positive cells.

AGE	DISTRIBUTION OF PCNA-POSITIVE CELLS		
	Cerebrum	Hippocampus	Cerebellum
E13	VZ (+++ /+++)		
E15	VZ (+++ / ++++)		
E18	VZ (~ SVZ) (+++/++++)		
E21	VZ ~ SVZ (++/++++)		EGL (++++/ ++~+)
P1	VZ ~SVZ (++/++++ ~+++)	SgZ (+ ~++ / ±)	EGL (++++/++)
P4	(VZ ~) SVZ (++ ~+ /+++)	SgZ (+ ~++ / ±)	EGL (+++ /++)
P7	(VZ ~) SVZ (+/+++ ~++)	SgZ (+ ~++ / ±)	EGL (++ ~++/++ ~+)
P14	(VZ ~) SVZ (+/+++ ~++)		EGL (++ ~+ / ++ ~+)
P21	(VZ ~) SVZ (+/++)		
P28	(VZ ~) SVZ (+ /+)		
P56	(VZ ~) SVZ (±/+)		
P84	(VZ ~) SVZ (±/+)		
P252	(VZ ~) SVZ (±/+)		

The percentage of PCNA-positive cells/the thickness in each layer. The percentage of PCNA positive cells: ++++; > 80%, +++; 50~80%, ++; 40~50%, +; 30~40%, ±; 30% >. Thickness of the layer is represented by cell number: ++++; > 15 cells, +++; 15~10cells, ++; 10~5cells, +; 5~2 cells, ±; 2 cells >.

mRNA signals (Figs. 3c, 4c, and 6a) including VZ, SVZ, and EGL. In some regions such as CP in embryonic days (Fig. 3c), cerebral cortex in neonatal days (Fig. 4a), Py, and IGL, no PCNA-positive cells were observed, although rpL4 signals were detected. PCNA-positive cells were observed in SgZ of the hippocampus, the lower zone of GCL, especially from P1 to P7. A very few PCNA-positive cells were also observed scattered in SgZ during postnatal days by P252 (not shown in Table 3).

Distribution of TUNEL-positive cells in the rat brain

The distribution of TUNEL-positive cells is summarized in Table 4. A small number of cells in VZ, SVZ (Figs. 3e, 4e) and EGL (Fig. 6c) were TUNEL-positive in embryonic to postnatal days. Few cells in the cerebral cortex from P1 to P21, IGL from P7 to P21, and hippocampus (GCL, and Py) from P1 to P4, were TUNEL-positive.

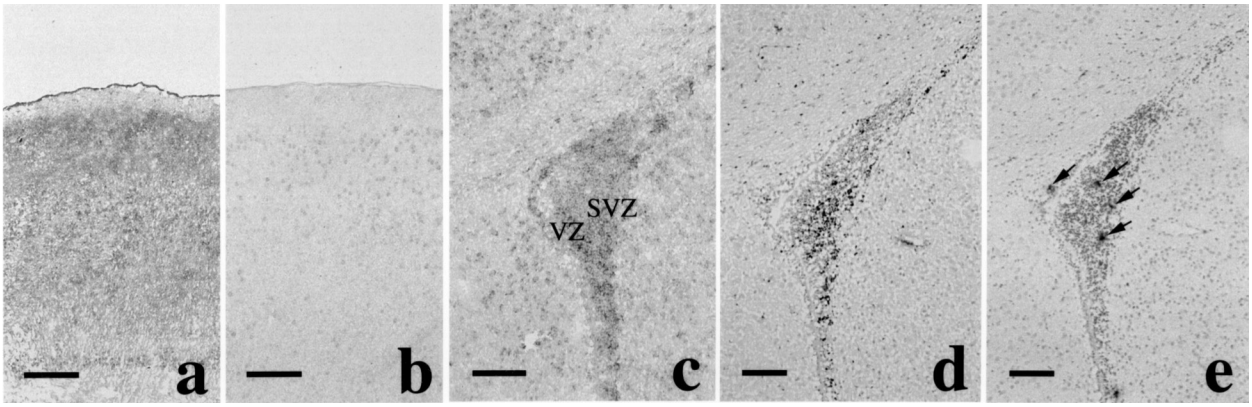

Fig. 4. Distribution of rpL4 mRNA and PCNA- or TUNEL-positive cells in the telencephalon of neonatal rats. Telencephalons at P4 **(a)**, P14 **(c, d, and e),** and P84 **(b)** are subjected to in situ hybridization **(a, b, and c)**, immunohistochemistry for PCNA (d) and TUNEL method (**e**; the arrows represent TUNEL-positive cells). Cortex (a and b) and VZ ~ SVZ **(c, d, and e)** are shown. Bar: a and b; 300 μm, c, d and e; 200 μm.

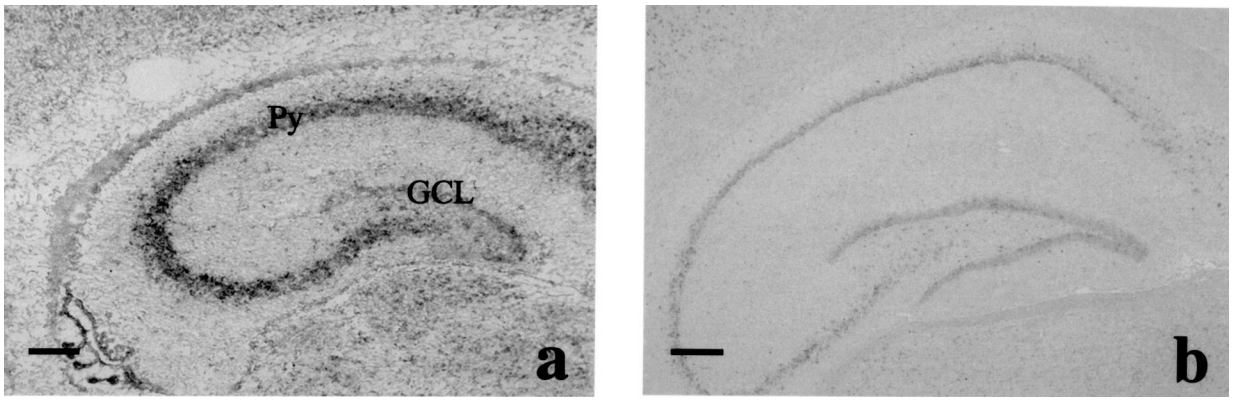

Fig. 5. Distribution of rpL4 mRNA in the hippocampus of neonatal rats. Hippocampi at P4 **(a)** and P84 **(b)** are subjected to in situ hybridization. Bar: a; 200 μm, b; 300 μm.

5AzC-induced rpL4 mRNA expression in the fetal brain

Intraperitoneal administration of 5AzC (10mg/kg) into pregnant rats at E13 induced apoptosis in the fetal brain. Apoptotic cells appeared at 9 HAT in VZ. The number of apoptotic cells reached its peak at 12HAT (Figs. 7,8), and slightly decreased at 24 HAT. On the other hand, the expression of rpL4 mRNA by RT-PCR method was unchanged up to 24 HAT (Fig. 9). The same results were obtained by *in situ* hybridization (data not shown).

Discussion

In the present study, we first examined the rpL4 expression in the developing rat brain. Remarkable rpL4

Table 4. The distribution of TUNEL-positive cells.

AGE	DISTRIBUTION OF TUNEL-POSITIVE CELLS			
	Cerebrum		Hippocampus	Cerebellum
E13	VZ (±)			
E15	VZ (±)			
E18	VZ~SVZ (±)	CP (-)		
E21	VZ~SVZ (±)	CP (-)		EGL (± ~ +)
P1	VZ~SVZ (±)	cortex (±)	GCL (± ~ +) Py (+)	EGL (+)
P4	VZ~SVZ (± ~ +)	cortex (± ~ +)	GCL (±) Py (± ~ +)	EGL (±)
P7	VZ~SVZ (± ~ +)	cortex (±)	GCL,Py (± ~ -)	EGL (±) IGL (+)
P14	VZ~SVZ (±)	cortex (±)	GCL,Py (± ~ -)	EGL (±) IGL (-)
P21	VZ~SVZ (±)	cortex (±)	GCL,Py (-)	EGL (±)
P28	VZ~SVZ (±)	cortex (- ~ ±)	GCL,Py (-)	IGL (-)
P56	VZ~SVZ (±)	cortex (- ~ ±)	GCL,Py (-)	IGL (-)
P84	VZ~SVZ (±)	cortex (-)	GCL,Py (-)	IGL (-)
P252	VZ~SVZ (±)	cortex (-)	GCL,Py (-)	IGL (-)

The percentage of TUNEL positive cells : + ; 1~3% , ± ; 0.1~0.3% , - ; 0~0.1%.

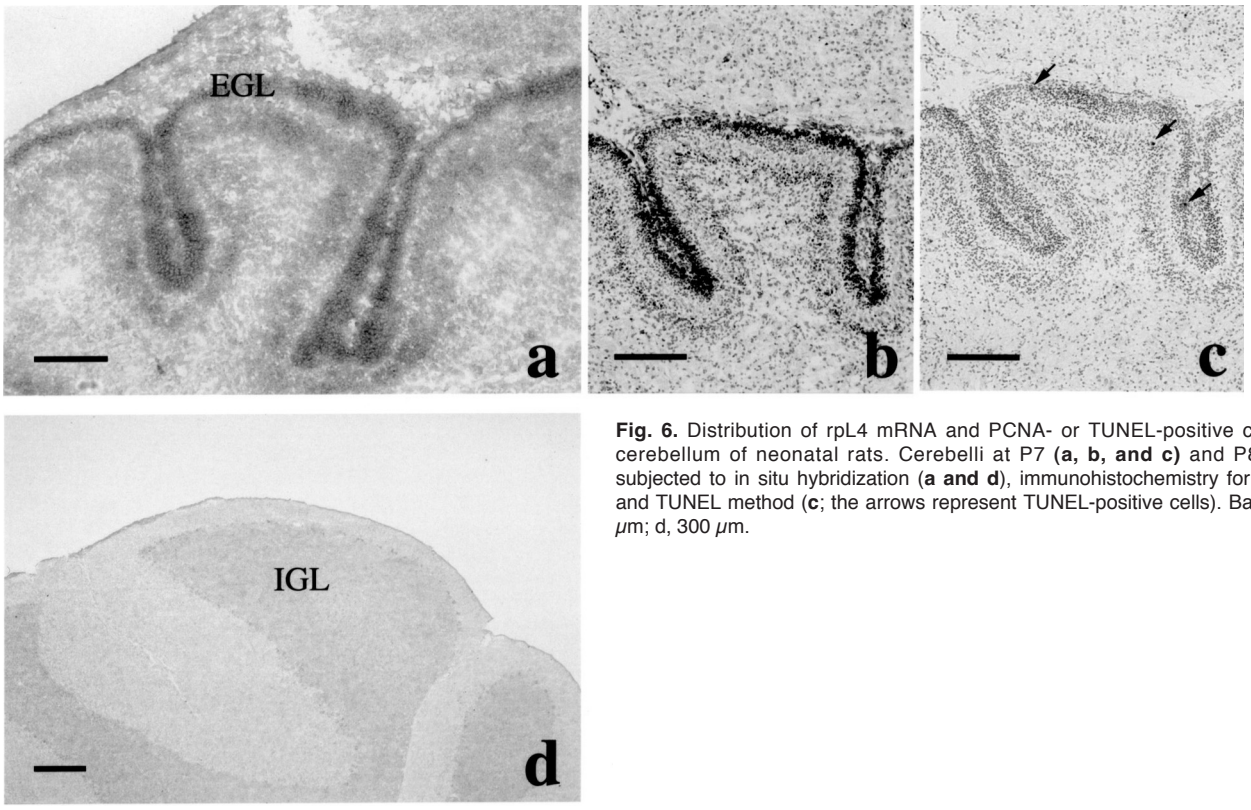

Fig. 6. Distribution of rpL4 mRNA and PCNA- or TUNEL-positive cells in the cerebellum of neonatal rats. Cerebelli at P7 **(a, b, and c)** and P84 **(d)** are subjected to in situ hybridization (**a and d**), immunohistochemistry for PCNA (b) and TUNEL method (**c**; the arrows represent TUNEL-positive cells). Bar: **a-c**; 200 μm; d, 300 μm.

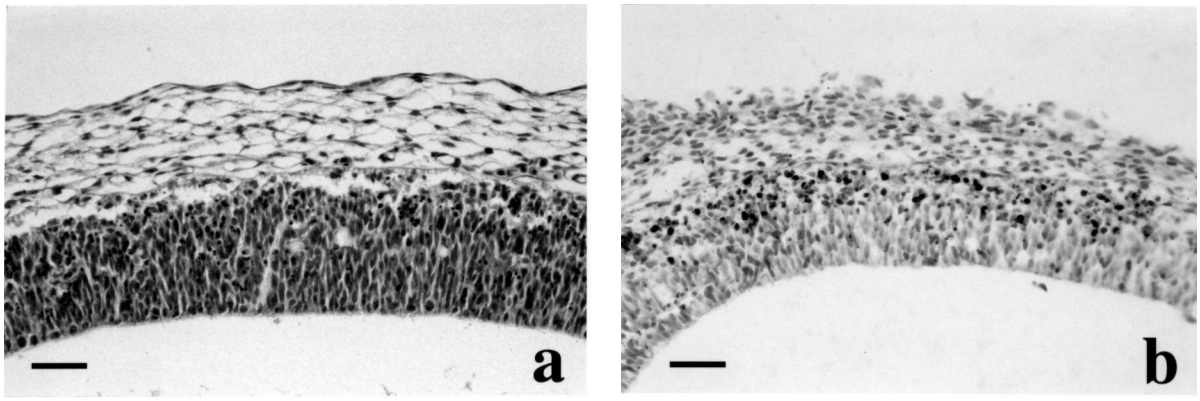

Fig. 7 Telencephalon of a 5AzC-treated fetus at 12HAT. A number of TUNEL-positive pycnotic cells are seen in VZ. **a:** HE stain, **b**: TUNEL method. Bar: 50 μm.

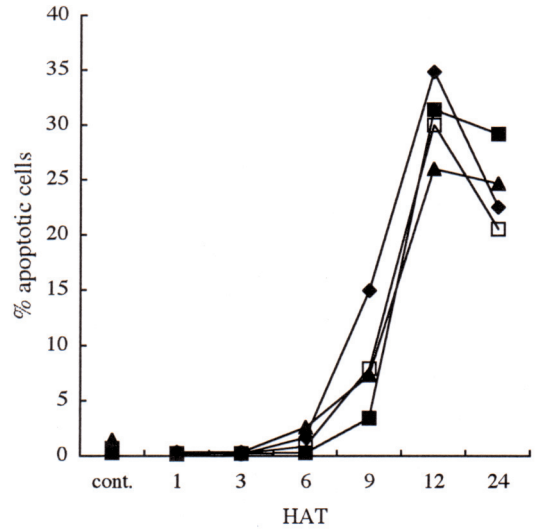

Fig. 8. Changes of % apoptotic cells in the brain of 5AzC-treated rat fetuses at E13. Mean of two dams are plotted. Black rhomb: telencephalon. Black square: diencephalon. Black triangle: mesencephalon. white square: metencephalon.

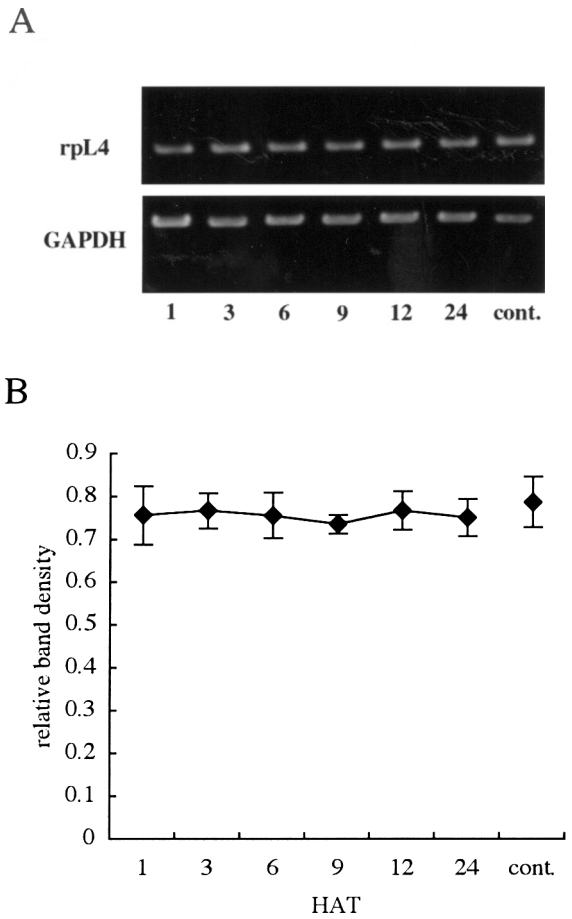

Fig. 9. Changes of rpL4 mRNA expression in the brain of 5AzC-treated rat fetuses at E13. **A.** RT-PCR products are electrophoresed in the agarose gel. **B.** The relative rpL4 band density to GAPDH is plotted (n=3). Mean±SD of 3 samples. No differences are shown between control and each value by Student's t -test.

expression in VZ, SVZ, and CP of the telencephalon were observed from E13 to E21, while they were weakened after P21. In the hippocampus, rpL4 was strongly expressed from P1 to P4, and decreased after P7. In the cerebellum, rpL4 was expressed in EGL from E21 to P14, and in IGL from P7 to P21. The aforementioned regions and periods in which rpL4 was expressed, corresponded to those in which neurons proliferate or differentiate.

In fact, in the present study, a number of PCNA-positive cells were observed in VZ and SVZ of the telencephalon during embryonic and neonatal days (from E13 to P14), and in cerebellular EGL by P14. It is well known that neuronal or glial progenitor cells proliferate

in VZ during embryonic days (Bayer and Altman, 1995a), SVZ during postnatal days (Luskin, 1993), and cerebellular EGL for 2 to 3 weeks after birth (Altman, 1972a). rpL4 mRNA, therefore, seems to be expressed in proliferating regions. Proliferating progenitor cells also exist in SgZ of hippocampus during postnatal days (Gage et al., 1998), which is observed as a few PCNA-positive cells by P252 in our experiment. However, it was difficult to recognize the progenitor cells on the sections subjected to *in situ* hybridization in the present study, and we were not able to correlate the rpL4 functions with the progenitor cells in SgZ.

On the other hand, the cerebral cortex, hippocampus, and cerebellular IGL in early postnatal days are the regions where neurons extensively differentiate. In the cerebral cortex, neurons which have migrated from VZ, spread neurites and form synaptic junctions of the adult levels and finish differentiation by P26 (Aghajanian and Bloom, 1967). Cerebellular granule cells have finished their migration from EGL to IGL by P20, and have completed differentiation by P21 (Altman, 1972b). Pyramidal cells in the hippocampus have finished their migration within few days after birth. In the dentate gyrus, proliferating cells are observed especially by P7, and thereafter they migrate to GCL where they differentiate (Bayer and Altman, 1995b). Therefore, rpL4 mRNA also seems to be expressed in differentiating regions.

From these results, a possible role of rpL4 during neurogenesis would be switching from proliferation to differentiation. However, there is also a possibility that the expression of rpL4 mRNA was elevated due to the elevated activity of ribosomes, which have a crucial role in protein synthesis. The protein synthesis and the activity of ribosomes seem to be high in the process of proliferation and differentiation. For clarifying the specific role of rpL4, further investigations on the expressions of other rps are needed.

On the other hand, it is inferred that rp may have another "extraribosomal function" such as regulation of cell growth or of apoptosis (Wool, 1996; Naora and Naora, 1999). In fact, there are some reports on extraribosomal rp functions involved in apoptosis. nbl (rpS3a) gene expression in the mouse thymus was increased in the process of glucocorticoid-induced apoptosis (Naora et al., 1995). rpS29 expression was elevated prior to adriamycin-induced apoptosis of rat thymocytes (Khanna et al., 2000). In Jurkat T-lymphoma cells, constitutive expression of rpL7 led to apoptosis (Neumann and Krawinkel, 1997). As mentioned before, we also reported that increased expressions of rpL4 preceded to 5AzC-induced apoptosis in PC12 cells (Kajikawa et al., 1998). Nevertheless, only few TUNEL-positive apoptotic cells could be detected in the brain of developing rats, and the regions of apoptotic cells did not correspond to those of rpL4 mRNA expression in the present study. Very small number of TUNEL-positive apoptotic cells in VZ, SVZ, and cerebral cortex during brain development have been reported (Thomaidou et al., 1997). rpL4 may not participate, at least, in the process of physiological apoptosis in the early phase of developing brain.

Secondly, we also examined the relationship between the expression of rpL4 mRNA and the development of 5AzC-induced neuronal apoptosis in the fetal brain. The expression of rpL4 could not be observed in the fetal brain where brain cell apoptosis was induced by 5AzC. The result is different from our previous report using PC12 cells *in vitro* (Kajikawa et al., 1998), in which the cells strongly expressed rpL4 mRNA prior to apoptosis. PC12 cells are derived from tumor cells (rat pheochromocytoma), basically not identical to normal brain cells. In addition, PC12 cells used in the previous study were not treated with nerve growth factor (NGF), not having neuronal features (undifferentiated). These differences of cell characteristics may account for the different rpL4 expression in the process of 5AzC-induced apoptosis. For confirming this possibility, 5AzC-induced rpL4 mRNA expression in NGF-treated PC12 cells and in cultured fetal neuronal cells should be examined.

References

Aghajanian G.K. and Bloom F.E. (1967). The formation of synaptic junctions in developing rat brain: a quantitative electron microscopic study. Brain Res. 6, 716-727.

Aloni R., Peleg D. and Meyuhas O. (1992). Selective translational control and nonspecific posttranscriptional regulation of ribosomal protein gene expression during development and regeneration of rat liver. Mol. Cell. Biol. 12, 2203-2212.

Altman J. (1972a). Postnatal development of the cerebellar cortex in the rat. 1. The external germinal layer and the transitional molecular layer. J. Comp. Neurol. 145, 353-397.

Altman J. (1972b). Postnatal development of the cerebellar cortex in the rat. 3. Maturation of the components of the granular layer. J. Comp. Neurol. 145, 465-513.

Bayer S.A. and Altman J. (1995a). Principles of neurogenesis, neuronal migration, and neural circuit formation. In: The rat nervous system. 2nd ed. Paxinos G. (ed). Academic Press. San Diego. pp 1079-1098.

Bayer S.A. and Altman J. (1995b). Neurogenesis and neuronal migration. In: The rat nervous system. 2nd ed. Paxinos G. Academic Press. San Diego. pp 1072-1074.

Bender C.M. Pao M.M. and Jones P.A. (1998). Inhibition of DNA methylation by 5-aza-2'-deoxycytidine suppresses the growth of human tumor cell lines. Cancer Res. 58, 95-101.

Chan Y.L., Olvera J. and Wool I.G. (1995). The primary structures of rat ribosomal proteins L4 and L41. Biochem. Biophys. Res. Commun. 214, 810-818.

Charache S., Dover G., Smith K., Talbot C.C. Jr., Moyer M. and Boyer S. (1983). Treatment of sickle cell anemia with 5-azacytidine results in increased fetal hemoglobin production and is associated with nonrandom hypomethylation of DNA around the gamma-delta-beta-globin gene complex. Proc. Natl. Acad. Sci. USA 80, 4842-4846.

Cheson B.D., Zwiebel J.A., Dancey J. and Murgo A. (2000). Novel therapeutic agents for the treatment of myelodysplastic syndromes. Semin. Oncol. 27, 560-577.

Constantinides P.G., Jones P.A. and Gevers W. (1977). Functional striated muscle cells from non-myoblast precursors following 5-azacytidine treatment. Nature 267, 364-366.

Gage F.H., Kempermann G., Palmer T.D., Peterson D.A. and Ray J. (1998). Multipotent progenitor cells in the adult dentate gyrus. J. Neurobiol. 36, 249-266.

Gavrieli Y., Sherman Y. and Ben-Sasson S.A. (1992). Identification of programmed cell death in situ via specific labeling of nuclear DNA fragmentation. J. Cell Biol. 119, 493-501.

Hara S., Tagawa Y., Ayabe H. and Darzynkiwicz Z. (1998). Analysis of drug-induced apoptosis in human leukemic cell line (HL-60). Gan to Kagaku Ryoho. Jpn. J. Cancer Chemother. 25, 393-399.

Hossain M.M., Nakayama H. and Goto N. (1995). Apoptosis in the central nervous system of developing mouse fetuses from 5-azacytidine-administered dams. Toxicol. Pathol. 23, 367-372.

Hossain M.M., Nakayama H. and Goto N. (1996). In vitro induction of apoptosis of developing brain cells by 5-azacytidine. Int. J. Dev. Neuroscience 14, 11-17.

Hossain M.M., Takashima A., Nakayama H. and Doi K. (1997a). 5-Azacytidine induces toxicity in PC12 cells by apoptosis. Exp. Toxicol. Pathol. 49, 201-206.

Hossain M.M., Nakayama H., Takashima A., Goto N. and Doi K. (1997b). 5-Azacytidine (5Az) induces apoptosis in PC12 cells: a model for 5Az-induced apoptosis in developing neuronal cells. Histol. Histopathol. 12, 439-445.

Kajikawa S., Nakayama H., Suzuki M., Takashima A., Murayama O., Nishihara M., Takahashi M. and Doi K. (1998). Increased expression of rat ribosomal protein L4 mRNA in 5-azacytidine-treated PC12 cells prior to apoptosis. Biochem. Biophys. Res. Commun. 252, 220-224.

Khanna N., Reddy V.G., Tuteja N. and Singh N. (2000). Differential gene expression in apoptosis: identification of ribosomal protein S29 as an apoptotic inducer. Biochem. Biophys. Res. Commun. 277, 476-486.

Lu D.P., Nakayama H., Shinozuka J., Uetsuka K., Taki R. and Doi K. (1998). 5-Azacytidine-induced apoptosis in the central nervous system of developing rat fetuses. J. Toxicol. Pathol. 11, 133-136.

Luskin M.B. (1993). Restricted proliferation and migration of postnatally generated neurons derived from the forebrain subventricular zone. Neuron 11, 173-189.

Michalowsky L.A. and Jones P.A. (1987). Differential nuclear protein binding to 5-azacytosine-containing DNA as a potential mechanism for 5-aza-2'-deoxycytidine resistance. Mol. Cell. Biol. 7, 3076-3083.

Murakami T., Li X., Gong J., Bhatia U., Traganos F. and Darzynkiewicz Z. (1995). Induction of apoptosis by 5-azacytidine: drug concentration-dependent differences in cell cycle specificity. Cancer Res. 55, 3093-3098.

Naora H., Nishida T., Shindo Y. and Adachi M. (1995). Association of nbl gene expression and glucocorticoid-induced apoptosis in mouse thymus in vivo. Immunology 85, 63-68.

Naora H. and Naora H. (1999). Involvement of ribosomal proteins in regulating cell growth and apoptosis: translational modulation or recruitment for extraribosomal activity? Immunol. Cell Biol. 77, 197-205.

Neumann F. and Krawinkel U. (1997). Constitutive expression of human ribosomal protein L7 arrests the cell cycle in G1 and induces apoptosis in Jurkat T-lymphoma cells. Exp. Cell Res. 230, 252-261.

Pinto A. and Zagonel V. (1993). 5-Aza-2'-deoxycytidine (Decitabine) and 5-azacytidine in the treatment of acute myeloid leukemias and myelodysplastic syndromes: past, present and future trends. Leukemia 7, 51-60.

Santi D.V., Norment A. and Garrett C.E. (1984). Covalent bond formation between a DNA-cytosine methyltransferase and DNA containing 5-azacytosine. Proc. Natl. Acad. Sci. USA 81, 6993-6997.

Sorm T.J., Piskala A. and Cihak A. (1964). 5-Azacytidine, a new highly effective cancerostatic. Experientia 20, 202-203.

Thomaidou D., Mione M.C., Cavanagh J.F. and Parnavelas J.G. (1997). Apoptosis and its relation to the cell cycle in the developing cerebral cortex. J. Neurosci. 17, 1075-1085.

Twiss J.L., Smith D.S., Chang B. and Shooter E.M. (2000). Translational control of ribosomal protein L4 mRNA is required for rapid neurite regeneration. Neurobiol. Dis. 7, 416-428.

Wang X.M., Wang X., Li J. and Evers B.M. (1998). Effects of 5-azacytidine and butyrate on differentiation and apoptosis of hepatic cancer cell lines. Ann. Surg. 227, 922-931.

Wool I.G., Chan Y.L. and Gluck A. (1995). Structure and evolution of mammalian ribosomal proteins. Biochem. Cell Biol. 73, 933-947.

Wool I.G. (1996). Extraribosomal functions of ribosomal proteins. Trends Biochem. Sci. 21, 164-165.

Accepted March 27, 2002